Proceedings of the 36th Chinese Control Conference
July 26-28, 2017, Dalian, China

Backstepping Control Design for UAV Formation With Input Saturation Constraint and Model Uncertainty

Zhong Zheng[1], Hui Yi[1]

1. College of Electrical Engineering and Control Science, Nanjing Tech University, Nanjing 210000, China
E-mail: zhengzhong8610@126.com
E-mail: jsyihui@126.com

Abstract: The novel backstepping control schemes are proposed to deal with the formation control problem of multiple unmanned aerial vehicles (UAVs) with input saturation constraint and model uncertainty. The trajectory tracking error model of the multiple UAVs formation is established. Then the standard ideal backstepping formation controller, which is applied to address the case with certain model and no input saturation constraint, is presented. After that, an adaptive backstepping controller associated with the designed command filter is developed to overcome input saturation constraint and model uncertainty. The controllers above enable the asymptotical Lyapunov stability of the closed-loop system. Numerical simulation results show that the proposed approaches are effective for the formation control of the UAV system.

Key Words: UAV formation, backstepping control, input saturation, asymptotical stability

1 Introduction

The recent few years have witnessed the burgeoning interest in maneuvering of unmanned aerial vehicles(UAVs) maintaining a geometric formation, due to its broad application such as surveillance, rescue missions, fire monitoring, operations in hazardous environments[1-4], to name a few. With the development of multi-agent control technologies, cooperative control of multiple UAVs becomes one choice for formation to satisfy military and civil task with high control accuracy, robustness and environmental adaptation.

A practical problem in the formation control of UAVs is the input saturation constraint. The actuators of the UAVs can usually afford limited control force, so it is essential to design the formation controller considering input saturation constraint in this sense. Backstepping control with command filter[5] is an effective tool to overcome the input saturation constraint problem. The filter structure can provide bounded output signals, which is helpful to conquer the input saturation problem. By incorporating the command filter, Farrel et al.[6] and Sonneveldt et al.[7] solve the input saturation problem in the adaptive flight control design. However, the design procedures are only applicable for the particular model in these literatures. Li et al.[8] presented an adaptive backstepping controller for optimal descent tracking. To overcome the input constraint, model uncertainties, and external disturbances, Zheng et al.[9] proposed robust adaptive backstepping control schemes for autonomous attitude cooperative of spacecraft formation. While, it should be noted that, the coordinated control of multiple UAVs formation with input constraint and model uncertainty, is not considered yet.

In this article, the backstepping formation control schemes of UAVs are proposed using command filter and adaptive technology. The rest of the paper is organized as follows. After providing the UAV formation model in Section 2, a standard backstepping control law for UAV formation is proposed in Section 3.1. After that, using the command filter design and adaptive control approach, we present the formation control law for UAVs to solve the problem with input constraint and model uncertainties in Section 3.2. Corresponding stability analysis is also provided. Numerical simulation results and conclusions are presented in Section 4 and Section 5 respectively.

2 Related Fundamental Theory

In this section, the kinematic and dynamic equations of the UAVs within a formation are given. Then the error models of the UAV system are also derived. For the formation system composed of n UAVs in 3-dimensional space, the kinematics of the ith UAV can be described by

$$\begin{aligned} \dot{x}_i &= V_i \cos\chi_i \cos\gamma_i \\ \dot{y}_i &= V_i \sin\chi_i \cos\gamma_i \\ \dot{z}_i &= V_i \sin\gamma_i \end{aligned} \tag{1}$$

where $i = 1, \cdots, n$ is the index of multiple UAVs, and n is the number of the UAVs. For the ith UAV, (x_i, y_i, z_i) is the position in the inertia frame, V_i is the speed, χ_i is the heading angle, γ_i is the flight path angle. The dynamics of the ith UAV can be described by

$$\begin{aligned} \dot{V}_i &= (T_i - D_i)/m_i - g\sin\gamma_i \\ \dot{\chi}_i &= L_i \sin\phi_i / (m_i V_i \cos\gamma_i) \\ \dot{\gamma}_i &= (L_i \cos\phi_i - m_i g \cos\gamma_i)/(m_i V_i) \end{aligned} \tag{2}$$

where T_i is the engine thrust, L_i and D_i are the vehicle lift and the drag, respectively. m_i, g and ϕ_i are the mass the gravitational constant and the banking angle, respectively. Let the control input $\boldsymbol{F}_i = \begin{bmatrix} T_i & L_i \sin\phi_i & L_i \cos\phi_i \end{bmatrix}^{\mathrm{T}}$, the position $\boldsymbol{p}_i = \begin{bmatrix} x_i & y_i & z_i \end{bmatrix}^{\mathrm{T}}$, and the velocity

*This work is supported by National Science Foundation of China under Grant 61503181, the Science Foundation of Jiangsu Province under Grant BK2010500.

$\boldsymbol{v}_i = \dot{\boldsymbol{p}}_i = \begin{bmatrix} \dot{x}_i & \dot{y}_i & \dot{z}_i \end{bmatrix}^{\mathrm{T}}$. Then from (1) and (2), it can be obtained that[10]

$$\begin{cases} \dot{\boldsymbol{p}}_i = \boldsymbol{v}_i \\ m_i \dot{\boldsymbol{v}}_i = \boldsymbol{\alpha}_i + m_i \boldsymbol{\varepsilon}_i + \boldsymbol{\beta}_i \boldsymbol{F}_i \end{cases} \tag{3}$$

where,

$$\boldsymbol{\alpha}_i = \begin{bmatrix} -D_i \cos\chi_i \cos\gamma_i \\ -D_i \sin\chi_i \cos\gamma_i \\ -D_i \sin\gamma_i \end{bmatrix} \tag{4}$$

$$\boldsymbol{\varepsilon}_i = \begin{bmatrix} 0 & 0 & g \end{bmatrix}^{\mathrm{T}} \tag{5}$$

$$\boldsymbol{\beta}_i = \begin{bmatrix} \cos\chi_i \cos\gamma_i & -\sin\chi_i & -\sin\gamma_i \cos\chi_i \\ \sin\chi_i \cos\gamma_i & \cos\chi_i & -\sin\chi_i \sin\gamma_i \\ \sin\gamma_i & 0 & \cos\gamma_i \end{bmatrix} \tag{6}$$

It is easy to find that the matrix $\boldsymbol{\beta}_i$ is invertible, and its inverse matrix is

$$\boldsymbol{\beta}_i^{-1} = \begin{bmatrix} \cos\chi_i \cos\gamma_i & \sin\chi_i \cos\gamma_i & \sin\gamma_i \\ -\sin\chi_i & \cos\chi_i & 0 \\ -\sin\gamma_i \cos\chi_i & -\sin\chi_i \sin\gamma_i & \cos\gamma_i \end{bmatrix} \tag{7}$$

In this paper, we need to design the cooperative formation controller to track the designed trajectory of each UAV.

In the formation maneuvering, the UAVs usually need to keep their formation shape. In this paper, the designed position of the *i*th UAV is denoted as $\boldsymbol{p}_i^d = \boldsymbol{p}_o^d + \boldsymbol{p}_{iF}$, where $\boldsymbol{p}_o^d$ is the desired position of the formation center, $\boldsymbol{p}_{iF}$ is the desired position of the UAV relative to the formation center. Note that $\boldsymbol{p}_i \to \boldsymbol{p}_i^d$ and $\dot{\boldsymbol{p}}_i \to \dot{\boldsymbol{p}}_i^d = \boldsymbol{v}_i^d$ mean that the formation tracking is satisfied, $\boldsymbol{p}_{oi} \to \boldsymbol{p}_{oj}$ and $\boldsymbol{v}_{oi} \to \boldsymbol{v}_{oj}$ mean that the formation keeping is satisfied. So the purpose of the paper is to design the UAV formation controllers $\boldsymbol{F}_i$ to track the designed trajectory of each UAV. In other word, $\boldsymbol{p}_i \to \boldsymbol{p}_i^d$ and $\dot{\boldsymbol{p}}_i \to \dot{\boldsymbol{p}}_i^d$ as $t \to \infty$.

3 Main Results

3.1 Backstepping Controller Design

The position and velocity tracking error are defined as $\boldsymbol{e}_{i1} = \boldsymbol{p}_i - \boldsymbol{p}_i^d$ and $\boldsymbol{e}_{i2} = \boldsymbol{v}_i - \boldsymbol{v}_i^d$. From (3), the error equations of the dynamic system are derived as

$$\dot{\boldsymbol{e}}_{i1} = \boldsymbol{e}_{i2} \tag{8}$$

$$m_i \dot{\boldsymbol{e}}_{i2} = \boldsymbol{\alpha}_i + m_i \boldsymbol{\varepsilon}_i + \boldsymbol{\beta}_i \boldsymbol{F}_i - m_i \ddot{\boldsymbol{p}}_i^d \tag{9}$$

Next, the standard backstepping control algorithms for the system (8)-(9) can be designed.

Backstepping is a recursive nonlinear control design approach. Its idea is to use part of system states as virtual controls to guarantee the stability of each recursive step.

Step 1: The first step in the backstepping involves control of the position of the UAVs by introducing a virtual velocity error. The first Lyapunov function candidate is selected as

$$V_1 = \frac{1}{2} \sum_{i=1}^{n} \boldsymbol{e}_{i1}^{\mathrm{T}} \boldsymbol{e}_{i1} \tag{10}$$

From (8), the derivative of V_1 can be obtained that

$$\dot{V}_1 = \sum_{i=1}^{n} \dot{\boldsymbol{e}}_{i1}^{\mathrm{T}} \boldsymbol{e}_{i1} = \sum_{i=1}^{n} \boldsymbol{e}_{i2}^{\mathrm{T}} \boldsymbol{e}_{i1} \tag{11}$$

The virtual velocity error is defined as

$$\boldsymbol{e}_{i3} = -k_1 \boldsymbol{e}_{i1} \tag{12}$$

where $k_1 > 0$ is a constant. The error between $\boldsymbol{e}_{i2}$ and $\boldsymbol{e}_{i3}$ is

$$\boldsymbol{z}_i = \boldsymbol{e}_{i2} - \boldsymbol{e}_{i3} = \boldsymbol{e}_{i2} + k_1 \boldsymbol{e}_{i1} \tag{13}$$

So it can be obtained that

$$\dot{V}_1 = \sum_{i=1}^{n} \boldsymbol{e}_{i2}^{\mathrm{T}} \boldsymbol{e}_{i1} = \sum_{i=1}^{n} \boldsymbol{z}_i^{\mathrm{T}} \boldsymbol{e}_{i1} - \sum_{i=1}^{n} k_1 \boldsymbol{e}_{i1}^{\mathrm{T}} \boldsymbol{e}_{i1} \tag{14}$$

Step 2: The second Lyapunov function candidate is chosen as

$$V_2 = \frac{1}{2} \sum_{i=1}^{n} m_i \boldsymbol{z}_i^{\mathrm{T}} \boldsymbol{z}_i + V_1 \tag{15}$$

The corresponding controller $\boldsymbol{F}_i$ is designed as

$$\boldsymbol{F}_i = \boldsymbol{\beta}_i^{-1} \left(-\boldsymbol{\alpha}_i - k_2 \boldsymbol{z}_i - \boldsymbol{e}_{i1} + m_i (\ddot{\boldsymbol{p}}_i^d - \boldsymbol{\varepsilon}_i - k_1 \boldsymbol{e}_{i2}) \right) \tag{16}$$

Then the derivative of V_2 can be written as

$$\begin{aligned} \dot{V}_2 &= \sum_{i=1}^{n} m_i \boldsymbol{z}_i^{\mathrm{T}} \dot{\boldsymbol{z}}_i + \dot{V}_1 \\ &= \sum_{i=1}^{n} \boldsymbol{z}_i^{\mathrm{T}} m_i (\dot{\boldsymbol{e}}_{i2} + k_1 \dot{\boldsymbol{e}}_{i1}) + \sum_{i=1}^{n} \boldsymbol{z}_i^{\mathrm{T}} \boldsymbol{e}_{i1} - \sum_{i=1}^{n} k_1 \boldsymbol{e}_{i1}^{\mathrm{T}} \boldsymbol{e}_{i1} \\ &= \sum_{i=1}^{n} \boldsymbol{z}_i^{\mathrm{T}} (\boldsymbol{\alpha}_i + m_i \boldsymbol{\varepsilon}_i + \boldsymbol{\beta}_i \boldsymbol{F}_i - m_i \ddot{\boldsymbol{p}}_i^d) + \\ &\quad \sum_{i=1}^{n} k_1 m_i \boldsymbol{z}_i^{\mathrm{T}} \boldsymbol{e}_{i2} + \sum_{i=1}^{n} \boldsymbol{z}_i^{\mathrm{T}} \boldsymbol{e}_{i1} - \sum_{i=1}^{n} k_1 \boldsymbol{e}_{i1}^{\mathrm{T}} \boldsymbol{e}_{i1} \\ &= -\sum_{i=1}^{n} k_2 \boldsymbol{z}_i^{\mathrm{T}} \boldsymbol{z}_i - \sum_{i=1}^{n} k_1 \boldsymbol{e}_{i1}^{\mathrm{T}} \boldsymbol{e}_{i1} \le 0 \end{aligned} \tag{17}$$

Now the backstepping control scheme of UAV formation is proposed. Further stability analysis will be carried out by Barbalat's Lemma in the proof of the following theorem.

Theorem 1. For the UAV formation control system (8)-(9), if the controller is designed as (16), the position and velocity tracking error $\boldsymbol{e}_{i1}$ and $\boldsymbol{e}_{i2}$ would converge to zero as the time goes to infinity.

Proof: Choose the Lyapunov function as (15). We can see that $\dot{V}_2 \le 0$, and $V_2 = 0$ if and only if $\boldsymbol{e}_{i1} = \boldsymbol{e}_{i2} = 0$. So the Lyapunov function V_2 is positive-definite. From (17), $V_2(t) \le V_2(0)$, so $\boldsymbol{e}_{i1}$ and $\boldsymbol{e}_{i2}$ are also bounded. From (9), (13) and (16), we can obtain that

$$m_i \dot{\boldsymbol{z}}_i = m_i \dot{\boldsymbol{e}}_{i2} + m_i k_1 \boldsymbol{e}_{i2} = -k_2 \boldsymbol{z}_i - \boldsymbol{e}_{i1} \tag{18}$$

So $\dot{\boldsymbol{z}}_i$ is also bounded. Differentiating (17), we can obtain that $\ddot{V}_2$ is bounded because $\boldsymbol{z}_i$, $\dot{\boldsymbol{z}}_i$, $\boldsymbol{e}_{i1}$ and $\dot{\boldsymbol{e}}_{i1}$ are all bounded. Therefore $\dot{V}_2$ is uniformly continuous. From Barbalat's Lemma[11], it concludes that V_2 converges to zero. So $\boldsymbol{z}_i$, $\boldsymbol{e}_{i1}$ and $\dot{\boldsymbol{e}}_{i1}$ converge to zero as the time goes to infinity.

3.2 Backstepping Controller with input saturation constraint and Uncertainty

It should be noted that we do not consider the problem of input saturation constraint and model uncertainty in Section 3.1. In practice, the actuators of UAVs can only apply

limited control force. If input saturation constraint is not considered in the design of the controller, the control effect might be bad, even the states of the closed-loop system could diverge to infinity. Besides, the parameters of the system model, such as the mass of the UAV, are often unavailable owing to fuel consumption or measure uncertainty. In this section, a command filtered adaptive backsteeping controller is proposed to overcome the input saturation constraint and model uncertainty problems.

Due to the constraint of input saturation, the controller is designed as

$$\boldsymbol{F}_i = \mathrm{sat}(\boldsymbol{f}_i) \tag{19}$$

where $\mathrm{sat}(\cdot)$ is the saturation function, which is defined as $\mathrm{sat}(\boldsymbol{y}) = [\mathrm{sat}(y_1) \quad \mathrm{sat}(y_2) \quad \mathrm{sat}(y_3)]^{\mathrm{T}}$ and

$$\mathrm{sat}(y_i) = \mathrm{sign}(y_i)\min\{y_0, |y_i|\} \tag{20}$$

for the vector $\boldsymbol{y} = [y_1 \quad y_2 \quad y_3]^{\mathrm{T}}$, $i = 1,2,3$, $y_0 > 0$ is the bound parameter of the saturation function. The auxiliary variable is defined as $\Delta\boldsymbol{f}_i = \boldsymbol{f}_i - \boldsymbol{F}_i$, and the virtual control $\boldsymbol{z}_{i1}$ and command filter $\boldsymbol{\xi}_i$ are respectively designed as

$$\boldsymbol{z}_{i1} = -k_1\boldsymbol{e}_{i1} + \boldsymbol{\xi}_i \tag{21}$$

$$\hat{m}_i\dot{\boldsymbol{\xi}}_i = -k_2\boldsymbol{\xi}_i + \boldsymbol{\beta}_i\Delta\boldsymbol{F}_i \tag{22}$$

where $k_1 > 0$, $k_2 > 0$, $\hat{m}_i$ denotes the estimation of the UAV mass m_i, $\boldsymbol{\beta}_i$ is defined in (6). The command filter (22) is used to compensate the effect of input saturation. Define

$$\boldsymbol{z}_{i2} = \boldsymbol{e}_{i2} - \boldsymbol{z}_{i1} = \boldsymbol{e}_{i2} + k_1\boldsymbol{e}_{i1} - \boldsymbol{\xi}_i \tag{23}$$

Substituting (23) into (9) and using (22), we can deduce that

$$\begin{aligned} m_i\dot{\boldsymbol{z}}_{i2} &= m_i\dot{\boldsymbol{e}}_{i2} + k_1 m_i\dot{\boldsymbol{e}}_{i1} - m_i\dot{\boldsymbol{\xi}}_i \\ &= \boldsymbol{\alpha}_i + m_i\boldsymbol{\varepsilon}_i + \boldsymbol{\beta}_i\boldsymbol{F}_i - m_i\ddot{\boldsymbol{p}}_i^d + k_1 m_i\boldsymbol{e}_{i2} - \tilde{m}_i\dot{\boldsymbol{\xi}}_i - \hat{m}_i\dot{\boldsymbol{\xi}}_i \\ &= \boldsymbol{\alpha}_i + m_i\boldsymbol{\varepsilon}_i + \boldsymbol{\beta}_i\boldsymbol{F}_i - m_i\ddot{\boldsymbol{p}}_i^d + k_1 m_i\boldsymbol{e}_{i2} - \tilde{m}_i\dot{\boldsymbol{\xi}}_i + k_2\boldsymbol{\xi}_i - \boldsymbol{\beta}_i\Delta\boldsymbol{F}_i \\ &= \boldsymbol{\alpha}_i + m_i\boldsymbol{H}_i + \boldsymbol{\beta}_i\boldsymbol{F}_i - \tilde{m}_i\dot{\boldsymbol{\xi}}_i + k_2\boldsymbol{\xi}_i - \boldsymbol{\beta}_i\Delta\boldsymbol{F}_i \\ &= \boldsymbol{\alpha}_i + m_i\boldsymbol{H}_i + \boldsymbol{\beta}_i\boldsymbol{f}_i - \tilde{m}_i\dot{\boldsymbol{\xi}}_i + k_2\boldsymbol{\xi}_i \end{aligned} \tag{24}$$

where $\tilde{m}_i = m_i - \hat{m}_i$, which denoted the deviation of UAV mass m_i and its estimated value $\hat{m}_i$, $\boldsymbol{H}_i = \boldsymbol{\varepsilon}_i - \ddot{\boldsymbol{p}}_i^d + k_1\boldsymbol{e}_{i2}$.

The control input and adaptive law are designed as

$$\boldsymbol{f}_i = \boldsymbol{\beta}_i^{-1}\left(-\boldsymbol{\alpha}_i - \hat{m}_i\boldsymbol{H}_i - k_2\boldsymbol{\xi}_i - k_3\boldsymbol{z}_{i2} - \frac{\boldsymbol{z}_{i2}}{\|\boldsymbol{z}_{i2}\|^2}\boldsymbol{e}_{i1}^{\mathrm{T}}(\boldsymbol{z}_{i2} + \boldsymbol{\xi}_i)\right) \tag{25}$$

$$\dot{\hat{m}} = \gamma_i\boldsymbol{z}_{i2}^{\mathrm{T}}(\boldsymbol{H}_i - \dot{\boldsymbol{\xi}}_i) \tag{26}$$

where the constant $\gamma_i > 0$.

Theorem 2: For the UAV formation control system (8)-(9), if the controller is designed as (19) and (25), the adaptive law is designed as (26), the command filter is designed as (21) and (22), and no input saturation occurs after finite time, then the position and velocity tracking error $\boldsymbol{e}_{i1}$ and $\boldsymbol{e}_{i2}$ will converge to zero as the time goes to infinity.

Proof: The Lyapunov function is defined as

$$V = \frac{1}{2}\sum_{i=1}^{n} m_i\boldsymbol{z}_{i2}^{\mathrm{T}}\boldsymbol{z}_{i2} + \frac{1}{2}\sum_{i=1}^{n}\boldsymbol{e}_{i1}^{\mathrm{T}}\boldsymbol{e}_{i1} + \frac{1}{2\gamma_i}\sum_{i=1}^{n}\tilde{m}_i^2 \tag{27}$$

We can see that the Lyapunov function $V \geq 0$, and V is a positive-definite function. Differentiating V and using (24)-(26) yield that

$$\begin{aligned} \dot{V} &= \sum_{i=1}^{n} m_i\boldsymbol{z}_{i2}^{\mathrm{T}}\dot{\boldsymbol{z}}_{i2} + \sum_{i=1}^{n}\boldsymbol{e}_{i1}^{\mathrm{T}}\dot{\boldsymbol{e}}_{i1} + \frac{1}{\gamma_i}\sum_{i=1}^{n}\tilde{m}_i\dot{\tilde{m}}_i \\ &= \sum_{i=1}^{n}\boldsymbol{z}_{i2}^{\mathrm{T}}(\boldsymbol{\alpha}_i + m_i\boldsymbol{H}_i + \boldsymbol{\beta}_i\boldsymbol{f}_i - \tilde{m}_i\dot{\boldsymbol{\xi}}_i + k_2\boldsymbol{\xi}_i) + \\ &\quad \sum_{i=1}^{n}\boldsymbol{e}_{i1}^{\mathrm{T}}\boldsymbol{e}_{i2} - \frac{1}{\gamma_i}\sum_{i=1}^{n}\tilde{m}_i\dot{\hat{m}}_i \\ &= \sum_{i=1}^{n}\boldsymbol{z}_{i2}^{\mathrm{T}}(\tilde{m}_i\boldsymbol{H}_i - \tilde{m}_i\dot{\boldsymbol{\xi}}_i - k_3\boldsymbol{z}_{i2}) - \sum_{i=1}^{n}\boldsymbol{e}_{i1}^{\mathrm{T}}(\boldsymbol{z}_{i2} + \boldsymbol{\xi}_i) + \\ &\quad \sum_{i=1}^{n}\boldsymbol{e}_{i1}^{\mathrm{T}}(\boldsymbol{z}_{i2} - k_1\boldsymbol{e}_{i1} + \boldsymbol{\xi}_i) - \sum_{i=1}^{n}\tilde{m}_i\boldsymbol{z}_{i2}^{\mathrm{T}}(\boldsymbol{H}_i - \dot{\boldsymbol{\xi}}_i) \\ &= -k_3\sum_{i=1}^{n}\boldsymbol{z}_{i2}^{\mathrm{T}}\boldsymbol{z}_{i2} - k_1\sum_{i=1}^{n}\boldsymbol{e}_{i1}^{\mathrm{T}}\boldsymbol{e}_{i1} \leq 0 \end{aligned} \tag{28}$$

So $\boldsymbol{z}_{i2}$, $\tilde{m}_i$ and $\boldsymbol{e}_{i1}$ are all bounded. The following proof is similar to the proof of Theorem 1. From (24) and (25), we obtain that

$$m_i\dot{\boldsymbol{z}}_{i2} = \tilde{m}_i\boldsymbol{H}_i - k_3\boldsymbol{z}_{i2} - \frac{\boldsymbol{z}_{i2}^{\mathrm{T}}}{\|\boldsymbol{z}_{i2}\|^2}\boldsymbol{e}_{i1}^{\mathrm{T}}(\boldsymbol{z}_{i2} + \boldsymbol{v}_i) - \tilde{m}_i\dot{\boldsymbol{v}}_i + k_2\boldsymbol{v}_i \tag{29}$$

So $\dot{\boldsymbol{z}}_i$ is also bounded. Differentiating (28), we can obtain that $\ddot{V}_2$ is bounded because $\boldsymbol{z}_{i2}$, $\dot{\boldsymbol{z}}_{i2}$, $\boldsymbol{e}_{i1}$ and $\dot{\boldsymbol{e}}_{i1}$ are all bounded. Therefore $\dot{V}_2$ is uniformly continuous. From Barbalat's Lemma[11], it concludes that V_2 converge to zero. So $\boldsymbol{z}_{i2}$ and $\boldsymbol{e}_{i1}$ converge to zero as the time goes to infinity.

If no input saturation occurs after finite time, that is to say, $\Delta\boldsymbol{F}_i = \boldsymbol{F}_i - \boldsymbol{f}_i = 0$ after a finite time T_0, from the command filter system Eq. (22) we can obtain that

$$\lim_{t\to\infty}\boldsymbol{v}_i(t) = 0 \tag{30}$$

Consequently, $\lim_{t\to\infty}\boldsymbol{e}_{i2}(t) = \lim_{t\to\infty}(\boldsymbol{z}_{i2}(t) - k_1\boldsymbol{e}_{i1}(t) + \boldsymbol{v}_i(t)) = 0$.

Remark: In Theorem 2, the assumption that no input saturation occurs after finite time must be satisfied in the proof. In fact, the closed-loop system cannot satisfy asymptotical stability if control input saturation constraints always exist as the time goes on. Generally, the causation of input saturation is the large initial position and velocity errors, and the control saturation constraints no longer occur after a long enough time in practice. So the assumption in Theorem 2 is reasonable to some extent.

4 Simulation Results

Simulation results are presented in this section to support the proposed methods. A scenario with four UAVs in the formation is considered. The UAVs in the formation aim to track the desired trajectory and maintain the square formation.

4.1 Simulation Settings

The mass of the UAVs are $m_1 = 150$ kg, $m_2 = 200$ kg, $m_3 = 180$ kg, $m_4 = 160$ kg, respectively. Let $\boldsymbol{p}_i = [x_i \quad y_i \quad z_i]^{\mathrm{T}}$, $\boldsymbol{w}_i = [V_i \quad \varphi_i \quad \gamma_i]^{\mathrm{T}}$, and the initial values of the $\boldsymbol{p}_i$ and $\boldsymbol{w}_i$ are given by

$$\boldsymbol{p}_1(0)=\begin{bmatrix}-58 & 62 & 584\end{bmatrix}^{\mathrm{T}}\ \mathrm{m},\ \boldsymbol{w}_1(0)=\begin{bmatrix}10 & 0 & 0\end{bmatrix}^{\mathrm{T}}\ \mathrm{m/s},$$
$$\chi_1(0)=0,\ \gamma_1(0)=0;$$
$$\boldsymbol{p}_2(0)=\begin{bmatrix}-62 & 60 & 580\end{bmatrix}^{\mathrm{T}}\ \mathrm{m},\ \boldsymbol{w}_2(0)=\begin{bmatrix}10 & 0 & 0\end{bmatrix}^{\mathrm{T}}\ \mathrm{m/s},$$
$$\chi_2(0)=0,\ \gamma_2(0)=0;$$
$$\boldsymbol{p}_3(0)=\begin{bmatrix}-60 & -60 & 416\end{bmatrix}^{\mathrm{T}}\ \mathrm{m},\ \boldsymbol{w}_3(0)=\begin{bmatrix}11 & 0 & 0\end{bmatrix}^{\mathrm{T}}\ \mathrm{m/s},$$
$$\chi_3(0)=0,\ \gamma_3(0)=0;$$
$$\boldsymbol{p}_4(0)=\begin{bmatrix}55 & 63 & 410\end{bmatrix}^{\mathrm{T}}\ \mathrm{m},\ \boldsymbol{w}_4(0)=\begin{bmatrix}11 & 0 & 0\end{bmatrix}^{\mathrm{T}}\ \mathrm{m/s},$$
$$\chi_4(0)=0,\ \gamma_4(0)=0;$$

The desired positions of the UAVs relative to the formation center are given by

$$\boldsymbol{p}_{1F}(0)=\begin{bmatrix}-60 & -60 & 60\sqrt{2}\end{bmatrix}^{\mathrm{T}}\ \mathrm{m},$$
$$\boldsymbol{p}_{2F}(0)=\begin{bmatrix}60 & 60 & 60\sqrt{2}\end{bmatrix}^{\mathrm{T}}\ \mathrm{m},$$
$$\boldsymbol{p}_{3F}(0)=\begin{bmatrix}-60 & -60 & -60\sqrt{2}\end{bmatrix}^{\mathrm{T}}\ \mathrm{m},$$
$$\boldsymbol{p}_{4F}(0)=\begin{bmatrix}60 & 60 & -60\sqrt{2}\end{bmatrix}^{\mathrm{T}}\ \mathrm{m}.$$

The desired position and velocity of the formation center are given by

$$\boldsymbol{p}_o^{\mathrm{d}}=\begin{bmatrix}0 & 100t & 500\end{bmatrix}^{\mathrm{T}}\ \mathrm{m},\ \boldsymbol{v}_o^{\mathrm{d}}=\dot{\boldsymbol{p}}_o^{\mathrm{d}}.$$

Then the desired position and velocity of each UAV are given by

$$\boldsymbol{p}_i^{\mathrm{d}}=\boldsymbol{p}_i^{F}+\boldsymbol{p}_o^{\mathrm{d}},\ \boldsymbol{v}_i^{\mathrm{d}}=\dot{\boldsymbol{p}}_i^{\mathrm{d}},\ i=1,2,3,4.$$

The controller parameters are chosen as

$$\lambda_1=1,\ k_i=3,\ \gamma_{m_i}=0.00001,\ \hat{m}_i(0)=100\ \mathrm{kg},$$
$$\boldsymbol{C}=\left[c_{ij}\right]_{4\times4}=\begin{bmatrix}0 & 0 & 0.1 & 0\\ 0.12 & 0 & 0 & 0\\ 0 & 0.1 & 0 & 0.08\\ 0.12 & 0 & 0 & 0\end{bmatrix}.$$

4.2 Simulation result Results

To describe the formation tracking and formation keeping performance of the UAVs quantitatively, the formation tracking error μ_1 and formation keeping error μ_2 are defined as

$$\mu_1=\frac{1}{4}\sum_{i=1}^{4}\left\|\boldsymbol{e}_i\right\|_2$$
$$\mu_2=\left|\left\|\boldsymbol{p}_1-\boldsymbol{p}_2\right\|_2-\left\|\boldsymbol{p}_1-\boldsymbol{p}_3\right\|_2\right|+\left|\left\|\boldsymbol{p}_1-\boldsymbol{p}_2\right\|_2-\left\|\boldsymbol{p}_3-\boldsymbol{p}_4\right\|_2\right|+\left|\left\|\boldsymbol{p}_2-\boldsymbol{p}_4\right\|_2-\left\|\boldsymbol{p}_3-\boldsymbol{p}_4\right\|_2\right|$$

According to the assignment of the desired formation configuration, it is obvious that smaller μ_1 and μ_2 during formation maneuver mean the better performance of formation tracking and formation maintenance.

The simulation results are given in Fig.1-Fig.3. The position tracking errors of the UAVs with the controller (19)-(22) are given in Fig. 1. We can see that the position tracking errors decay quickly as the time goes on. From Fig.2, the velocity tracking errors of the UAVs also converge to zero as the time goes on. So the purpose of tracking the desired trajectory and maintaining the desired square formation is satisfied. Fig.3 shows the formation-keeping error μ_1 and formation keeping error μ_2. It can be seen that μ_1 and μ_2 can also converge to zero, which implies the well formation-tracking and formation-keep performance. Therefore the simulation results demonstrate the validation of the presented controllers.

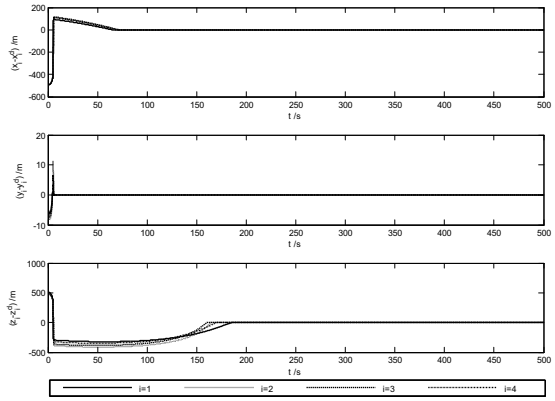

Fig.1: Position tracking errors of UAVs

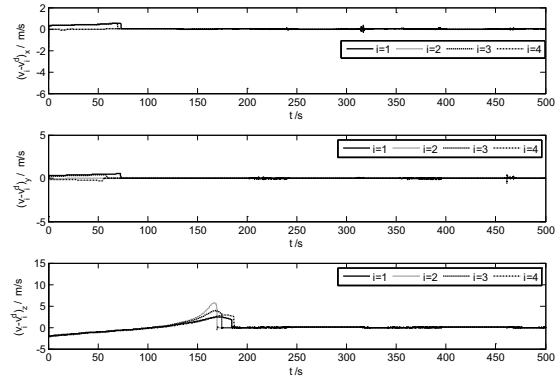

Fig.2: Velocity tracking errors of UAVs

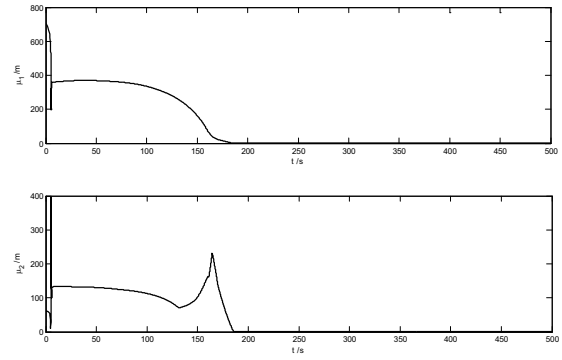

Fig. 3: Formation-tracking error and formation-keeping error of UAVs

5 Conclusion

The primary contribution of this study lies in the development and stability analysis of the backstepping control associated with the command filter for UAV formation. A standard backstepping control strategy is introduced to solve the problem with certain model parameters and no input saturation constraint. An adaptive backstepping formation controller with an appropriate command filter is proposed to overcome the problem of input saturation constraint and model uncertainty. The

asymptotical stability analysis method is given by choosing a reasonable Lyapunov function. Also the simulation results validate the well performance of the developed methods.

References

[1] F. Giulietti, L. Pollini, M. Innocenti, Autonomous formation flight, *IEEE Control Systems Magazine*, 20(6): 34–44f, 2000.

[2] A. dogan, S. Venkataramanan, Nonlinear control for reconfiguration of unmanned-vehicle formation, *Journal of Guidance, Control, and Dynamics*, 28(4): 667–678, 2005.

[3] J. Shan, H. T. Liu, Close-formation flight control with motion asnchronization, *Journal of Guidance, Control, and Dynamics*, 28(6): 1316–1320, 2005.

[4] D. W. Dai, H. Y. Long, Development and application of unmanned aerial vehicle, *Command Information System and Technology*, 4(4): 7–10, 2013.

[5] J. Farrell, M. Polycarpou, M. Sharma, et al, Command filtered backstepping, *IEEE Transactions on Automatic Control*, 54(6): 1391–1395, 2009.

[6] J. Farrell, M. Polycarpou, M. Sharma, Backstepping-based flight control with adaptive function approximation, *Journal of Guidance, Control, and Dynamics*, 28(6): 1089–102, 2005.

[7] L. Sonneveldt, Q. P. Chu, J. A. Mulder, Nonlinear flight control design using constrained adaptive backstepping, *Journal of Guidance, Control, and Dynamics*, 30(2): 322–36, 2007.

[8] M. Li, W. Jing, M. Macdonald, et al, Adaptive backstepping control for optimal descent with embedded autonomy, *Aerospace Science and Technology*, 13(3): 589–94, 2011.

[9] Z. Zheng, S. Song, Autonomous attitude coordinated control for spacecraft formation with input constraint, model uncertainties, and external disturbances, *Chinese Journal of Aeronautics*, 27(3): 602–612, 2014.

[10] S. Kim, Y. Kim, Three dimensional optimum controller for multiple UAV formation flight using behavior-based decentralized approach, *Control, Automation and Systems, International Conference on IEEE*, 1387–1392, 2007.

[11] H. Khalil, *Nonlinear Systems*. New Jersey: Prentice-Hall, 2002, 3rd edition.